10-1-1999

Simultaneous photometry and spectroscopy of the newly discovered γ Doradus variable HR 8330=HD 207223

Anthony B. Kaye
Los Alamos National Laboratory

Gregory W. Henry
Tennessee State University

Francis C. Fekel
Tennessee State University

Douglas S. Hall
Vanderbilt University

Recommended Citation

Anthony B. Kaye, Gregory W. Henry, Francis C. Fekel, Douglas S. Hall, Simultaneous photometry and spectroscopy of the newly discovered γ Doradus variable HR 8330=HD 207223, Monthly Notices of the Royal Astronomical Society, Volume 308, Issue 4, October 1999, Pages 1081–1086, https://doi.org/10.1046/j.1365-8711.1999.02768.x

Mon. Not. R. Astron. Soc. **308**, 1081–1086 (1999)

Simultaneous photometry and spectroscopy of the newly discovered γ Doradus variable HR 8330 = HD 207223

Anthony B. Kaye,[1★] Gregory W. Henry,[2] Francis C. Fekel[2★] and Douglas S. Hall[3]

[1]*Los Alamos National Laboratory, X-TA, MS B-220, Los Alamos, NM 87545, USA*
[2]*Center of Excellence in Information Systems, Tennessee State University, 330 10th Ave. North, Nashville, TN 37203, USA*
[3]*Dyer Observatory, Vanderbilt University, 1000 Oman Drive, Brentwood, TN 37027, USA*

Accepted 1999 May 7. Received 1999 May 4; in original form 1998 September 2

ABSTRACT

We present *BV* photometry and simultaneous high-resolution, high signal-to-noise ratio spectroscopy of the newly-discovered γ Doradus variable HR 8330 taken during the 1997 and 1998 observing seasons. We calculate power spectra for the *B*- and *V*-band data sets and for the time series defined throughout the observing season at each point across the Fe II λ4508.289 and the Ti II λ4501.278 line profiles to search for periodic variability. Period analysis reveals a single, 2.6-d period in both the photometric and the spectroscopic data, with a 237° phase lag between them. Based on the location of HR 8330 in the HR diagram and the characteristics of its photometric and spectroscopic variations, we conclude that HR 8330 is a bona fide γ Doradus-type pulsating variable.

Key words: stars: activity – stars: individual: HR 8330 – stars: oscillations – stars: variables: other.

1 INTRODUCTION

Informal discussions at the 'Astrophysical Applications of Stellar Pulsation' conference (Stobie & Whitelock 1995) held in 1995 in Cape Town, South Africa led to the conclusion that a group of approximately one dozen newly-discovered variables formed a reasonably homogeneous group that constituted a new class of variable stars. These new variables cluster around spectral type F0 and luminosity class V or IV-V. They are generally young and have solar or subsolar metallicities. Typical periods range from 0.4–3 d; associated amplitudes can be as large as 0.1 mag in *V* and several km s^{-1} in radial velocity. However, the particular physical mechanism driving the photometric and spectroscopic variations has been a matter of conjecture. Currently, the most likely mechanism is thought to be photospheric non-radial pulsations (NRP) (see, e.g., Krisciunas et al. 1993, 1995; Balona et al. 1996; Zerbi et al. 1997; Kaye 1998).

HR 8330 (= HD 207223; $m_V = 6.2$) was first recognized as a low-amplitude variable by one of us (GWH) after it was chosen as a comparison star for high-precision photometry of solar-type stars with the Smithsonian Astrophysical Observatory/Tennessee State University 0.75-m Automatic Photoelectric Telescope (APT) (Henry 1995). Preliminary results on its photometric and spectroscopic variations were given by Kaye (1998). In this paper, we present a detailed analysis of our *BV* photometry and simultaneous high-resolution, high signal-to-noise ratio (S/N) spectroscopy of the star acquired during the 1997 and 1998 observing seasons. We also derive the observed phase lag between the spectroscopy and the photometry and discuss possible physical scenarios capable of explaining the observations.

2 OBSERVATIONS

Time-series analysis of γ Doradus stars can be quite difficult when only single-site data are available. This is mainly because the periods of variation in both the photometry and the spectroscopy are often close to one day. The signal measured by the observer at the telescope is the convolution of the 'true' signal(s) from the star and the 'window' signal imposed by the pattern of the observations. No matter how many data points are taken each night, the true signal will be seen only after extended observing runs that have data spread out over many consecutive nights.

Secondly, the density of blended lines in the spectrum makes time-series analysis of line profiles in F-type dwarfs difficult for the optical observer. With this in mind, a section of the spectrum with a few reasonably unblended, isolated metallic lines between 4500 and 4520 Å was chosen. Even in this relatively restricted region, the Ti II λ4501.278 line and the Fe II λ4508.289 line are the only lines suitable for analysis.

2.1 Photometry

Differential *BV* photometry was taken during the second, third,

★ Visiting Astronomer, Kitt Peak National Observatory, National Optical Astronomy Observatories, which is operated by the Association of Universities for Research in Astronomy, Inc. (AURA) under cooperative agreement with the National Science Foundation.

and fourth quarters of 1997 and during the first and second quarters of 1998 (JD 245 0563–245 0998) with the 0.4-m APT operated jointly by Vanderbilt University and Tennessee State University and located in Washington Camp, Arizona.

Each differential magnitude reported in this paper is the mean of three intercomparisons between the variable and comparison stars in the sense variable minus comparison, where HD 209166 ($m_V = 5.60$, $B - V = 0.34$, F4 III) is the comparison star. A mean is rejected if its internal uncertainty exceeds 0.01 mag, this being the procedure to remove measurements made when sky conditions are not photometric. All data have been corrected for differential atmospheric extinction and transformed to the Johnson *UBVRI* standard photometric system; all times are heliocentric. Observations were obtained each night at hour angles of −4, −2, 0, +2, and +4, resulting in a total of 302 *V* and 298 *B* means for the 1997 and 1998 observing seasons. The star HD 204277 ($m_V = 6.72$, $B - V = 0.50$, F8 V) was also observed as a check star; differential magnitudes between the check and comparison stars reveal both are constant to 0.006 mag or better.

Further details on the 0.4-m APT as well as the observing and data reduction procedures can be found in Henry (1995).

2.2 Spectroscopy

Seventy-six high S/N spectra were obtained over 11 nights at the Kitt Peak National Observatory during 1997 late November and early December, with the 0.9-m coudé feed telescope. These spectra were taken simultaneously with photometry obtained at Washington Camp, Arizona.

Each spectrum covers the wavelength region 4403 to 4617 Å, has a resolution of 0.18 Å, and was obtained using grating A, camera 5, and the long collimator. Filter 4-96 was used to block both higher and lower orders. Data were recorded on the F3KB CCD (3000 × 1000 pixel, 15 × 15 μm pixel size, 75 per cent detector quantum efficiency at 4210 Å). A typical exposure time for spectra in this region was 900 s, resulting in a S/N of approximately 325. Th–Ar exposures used for wavelength calibration were taken immediately before and after each stellar exposure.

In addition to the large number of blue-wavelength spectra, on 1996 October 5, one spectrum was obtained at red wavelengths with the coudé feed telescope, coudé spectrograph, grating A, camera 5, and a TI CCD. The spectrum is centred at 6430 Å, has a wavelength range of over 80 Å, and a resolution of 0.21 Å.

All spectra were reduced at the National Optical Astronomy Observatories offices in Tucson, Arizona in the standard fashion using IRAF[1] and included optimal aperture extraction, bias subtraction, and flat field division. The spectra were rectified to a unit continuum by fitting a straight line through known continuum regions and were put on a uniform heliocentric wavelength grid.

3 BASIC PROPERTIES

The spectral type of HR 8330 was determined by visually comparing its red wavelength spectrum to spectra of late-A and early-F stars (Fekel 1997) that had well-determined spectral types by reliable classifiers. The standards were obtained with the same telescope, spectrograph, and detector setup as our red spectrum of HR 8330. We classify the spectrum as F2 V, which is in excellent agreement with the F3 V spectral type of Cowley (1976). In the 6430-Å region, the rotational broadening and line strengths of HR 8330 are nearly identical to those of HR 6844 (F1 V, Gray & Garrison 1989), which has [Fe/H] = 0.17 (Boesgaard & Tripicco 1986).

[1] IRAF is distributed by the National Optical Astronomy Observatories, which is operated by the Association of Universities for Research in Astronomy, Inc., under contract to the National Science Foundation.

Table 1. HR 8330: basic properties.

Quantity	Value	Reference
m_V	6.18	(1)
$B - V$	0.35	(1)
π	0.01990 ± 0.0008 arcsec	(1)
$T_{\rm eff}$	7047 K	(2)
Spectral type	F2 v	
$v \sin i$	9.1 ± 1.0 km s^{-1}	
M_V	2.62 ± 0.09	
L	6.88 ± 0.56 $L_\odot$	
R	1.76 ± 0.10 $R_\odot$	
M	1.5 ± 0.2 $M_\odot$	(3)
$\log g$	4.12 ± 0.08	
estimated [Fe/H]	0.15 ± 0.10	

(1) ESA (1997); (2) Flower (1996); (3) Gray (1992).

The radial velocity of the red wavelength spectrum was determined by cross-correlation with HR 7560, the velocity of which was assumed from Scarfe, Batten & Fletcher (1990). The velocity of −21.9 km s^{-1} for HR 8330 is consistent with the value of −19.7 km s^{-1} found from four observations at David Dunlap Observatory (Young 1945).

Using the procedure and empirical relation of Fekel (1997) and a macroturbulence of 5 km s^{-1} (Gray 1982), we derive $v \sin i = 9.1 \pm 1.0$ km s^{-1}.

The Strömgren and Hβ photometry of Crawford et al. (1966) for HR 8330 and the empirical relations determined by Crawford (1975) for F stars are used to compute additional properties. The quantities $\delta c_1(\beta) = 0.087$ and $\delta m_1(\beta) = 0.009$ reveal that HR 8330 is only 0.8 mag above the zero-age main sequence (ZAMS) and somewhat metal rich.

The *Hipparcos* parallax, absolute *V* magnitude, and $B - V$ colour (ESA 1997), combined with the relations of Flower (1996), enable basic parameters to be determined for HR 8330. These basic properties are summarized in Table 1. References are given for the adopted quantities, while quantities without a reference have been computed or estimated in the present work. $M_V = 2.44$, as determined from Strömgren photometry, is less than 0.2 mag brighter than that determined from the *Hipparcos* parallax (Table 1) and, thus, is in excellent agreement.

These results show that HR 8330 is an early-F dwarf but somewhat evolved from the ZAMS. Both spectroscopy and photometry suggest [Fe/H] ∼ 0.1–0.2, making HR 8330 more metal rich than the Sun.

4 DATA ANALYSIS

We chose to perform our time-series analysis by means of Vaniček's (1971) least-squares method. This method does not depend upon prewhitening and is particularly suitable when, as in the present case, signals at low frequencies are expected. This method has been used in the data analysis of a variety of other γ Doradus stars, most recently for HR 8799 (Zerbi et al. 1999).

4.1 Photometric results

Operation of the APT ceases during the summer months because

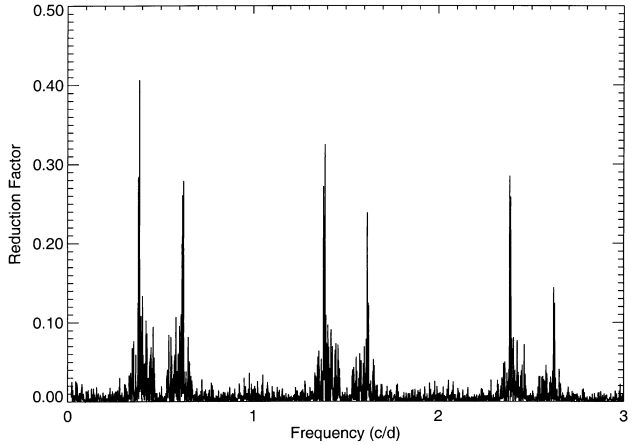

Figure 1. A power spectrum of the complete *B*-band photometric data set showing a single frequency ($\nu = 0.385\,53\,\mathrm{d}^{-1}$) and its one cycle per day aliases.

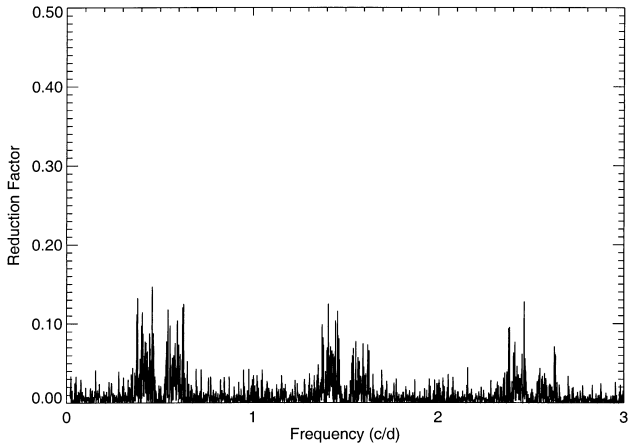

Figure 2. A power spectrum of the complete *B*-band photometric data set after removal of the $\nu = 0.385\,53\,\mathrm{d}^{-1}$ signal.

Table 2. HR 8330: results obtained from photometric data.

Data Group, Band pass	Date Range *HJD*-2450000.	*n*	Period (*d*)	Frequency (d^{-1})	Amplitude (mmag)	T_p *HJD*-2450000.
A, *V*	563–643	88	2.6086	0.3833	25.6	600.222
			±0.0049	±0.0007	±1.4	±0.046
A, *B*	563–643	87	2.6070	0.3836	31.4	600.259
			±0.0044	±0.0006	±1.5	±0.040
B, *V*	712–816	152	2.6125	0.3828	14.6	758.368
			±0.0074	±0.0011	±0.9	±0.054
B, *B*	712–816	148	2.6138	0.3826	22.0	758.418
			±0.0052	±0.0008	±1.1	±0.042
C, *V*	929–998	62	2.5995	0.3847	19.2	958.166
			±0.0067	±0.0010	±1.4	±0.053
C, *B*	929–998	63	2.6051	0.3839	25.8	958.105
			±0.0061	±0.0009	±1.7	±0.048
D, *V*	563–998	302	2.59411	0.38549	17.6	758.426
			±0.00059	±0.00009	±0.7	±0.033
D, *B*	563–998	298	2.59381	0.38553	23.6	758.450
			±0.00052	±0.00008	±0.8	±0.029

photometric sky conditions are rare during the southern Arizona rainy season. Therefore, the data for HR 8330 naturally divide into two separate groups within each observing season. The data reported in this paper were taken in the 1997 and 1998 observing seasons and are divided into groups **A**, **B**, and **C**.

Fourier analysis of each data group reveals a single period present in both the *B* and *V* data sets within each group. The period is constant (within formal errors) over the entire course of the observations, while the amplitude shows 2–3σ variations. Thus, we are able to create one large data set (**D**) that is the concatenation of the three smaller sets. Fig. 1 shows the power spectrum of the complete *B*-band data set, clearly displaying a single strong frequency and its aliases. Once this frequency is removed, the data show no other statistically significant frequencies (Fig. 2).

Table 2 presents the results of our frequency analysis of the 600 photometric measurements. Column 1 lists the data group and bandpass. Columns 2 and 3 give the HJD range and number of observations in each data group, respectively. Columns 4 and 5 list the periods and corresponding frequencies found in each group. Column 6 gives the (peak-to-peak) amplitudes. Column 7 lists T_{p}, a time of photometric minimum light near the middle of the data set, assuming each periodicity can be modelled as a pure sine curve. We adopt a weighted mean of the *B* and *V* bandpass solutions from data set **D** to be our final photometric solution:

$$T_{\mathrm{p}} = 2\,450\,758.440 \pm 0.022\,\mathrm{d}, \qquad P = 2.593\,96 \pm 0.00059\,\mathrm{d}.$$

Fig. 3 shows the data plotted modulo the weighted-mean period. The rms scatter of the observations from a pure sine curve is 0.0092 mag. This is somewhat larger than the 0.003–0.004 mag precision of the observations made with the 0.4-m APT (Henry 1995). The additional scatter is likely to be the result of the presence of the 2–3σ variations in the photometric amplitude from data set to data set seen in Table 2 and the possibility that the variations may not be purely sinusoidal.

4.2 Spectroscopic results

In stars for which line profile variations are absent, the photospheric lines are typically symmetric and, as such, the centroid, median, and mode of each line profile coincide. In such cases, the method of cross-correlation is able to provide accurate radial-velocity measurements. However, in stars displaying line profile variations (e.g., pulsating stars or spotted stars), the line profiles are typically asymmetric and so the displacement of the line needs to be carefully defined. We have chosen to measure the displacement of the line profile relative to the rest wavelength of

the line (a quantity closely related to the radial velocity) using the so-called first moment of the line profile (see Balona 1987; Aerts 1996),

$$M_1 = \frac{\sum \lambda \times I_\lambda}{\sum I_\lambda}, \quad (1)$$

where I_λ represents the intensity of the line profile (after subtraction of the continuum and inversion of the profile) at each wavelength λ.

From the moments, we determine relative radial velocities corrected for the Earth's motion for the Fe II λ4508.289 and Ti II λ4501.279 lines, which were the only unblended lines in our blue wavelength spectra. Those velocities have been used to determine the period and amplitude of the line-profile variations with the method of Vaniĉek (1971). Table 3 details the results of the analysis performed on the blue-wavelength spectra. Columns 1, 2 and 3 list the spectral line, HJD range, and number of velocities. Column 4 gives the period determined for the Fe II and Ti II data sets. Columns 5 and 6 list the amplitude of the variation (in $\mathrm{km\,s^{-1}}$) and the time of zero radial velocity on the ascending part of the radial velocity curve, which we define as T_v. We adopt the following weighted-mean values as our final spectroscopic solution:

$$T_v = 2\,450\,780.078 \pm 0.013\,\mathrm{d}, \qquad P = 2.61 \pm 0.04\,\mathrm{d}.$$

Fig. 4 shows the Fourier analysis of the Fe II λ4508.289 line profile as a function of both time and position across the line profile. The bottom panel is a plot of the global average line profile, plotted as intensity versus velocity. The top panel is a 'normal' periodogram (i.e., frequency is plotted on the upper ordinate), but now also shows signal *strength* as a function of position across the line profile. The strength of each signal is shown by the grey-scale in which darker shades indicate a stronger signal. There are no strong periodic signals detected other than the dominant frequency. This periodogram was passed through 10 iterations of the CLEAN algorithm (Högbom 1974) using a gain of 0.9. Note the excellent agreement between the results obtained from the spectroscopy and the photometry.

We present the radial velocities calculated from the first moments of the Fe II λ4508.289 line profile phased with the 2.61-d period in Fig. 5. It appears that there may be additional, more rapid radial velocity variations, not apparent in the photometry. This suggests that weak, higher-degree ($\ell > 4$) pulsations may be present. However, additional frequency analysis of the radial velocities extended to a maximum frequency of $30\,\mathrm{d^{-1}}$ (which would show high ℓ variations if they were present) does not reveal another periodicity.

4.3 Phase lag

Since the photometric and the spectroscopic data have the same period, we can check the phasing between the two data sets. As in the case of adiabatic pulsation (see Cox 1980), we define zero phase lag, $\Delta\phi \equiv 0$, when the time of maximum brightness coincides with the time of minimum radius. This is equivalent to

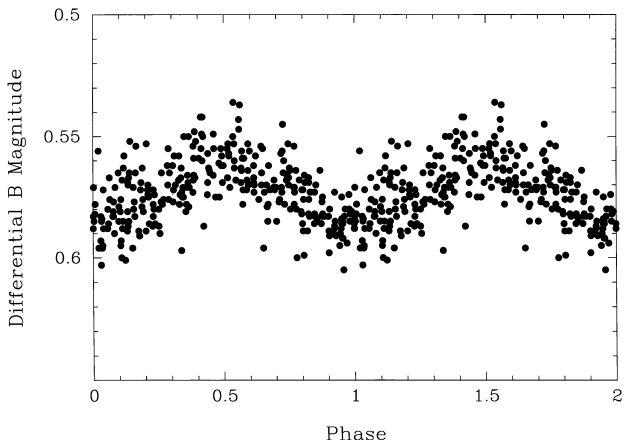

Figure 3. The complete *B*-band data set phased with the weighted mean values $T_p = 2\,450\,758.440$ and $P = 2.593\,96\,\mathrm{d}$ determined from Table 2.

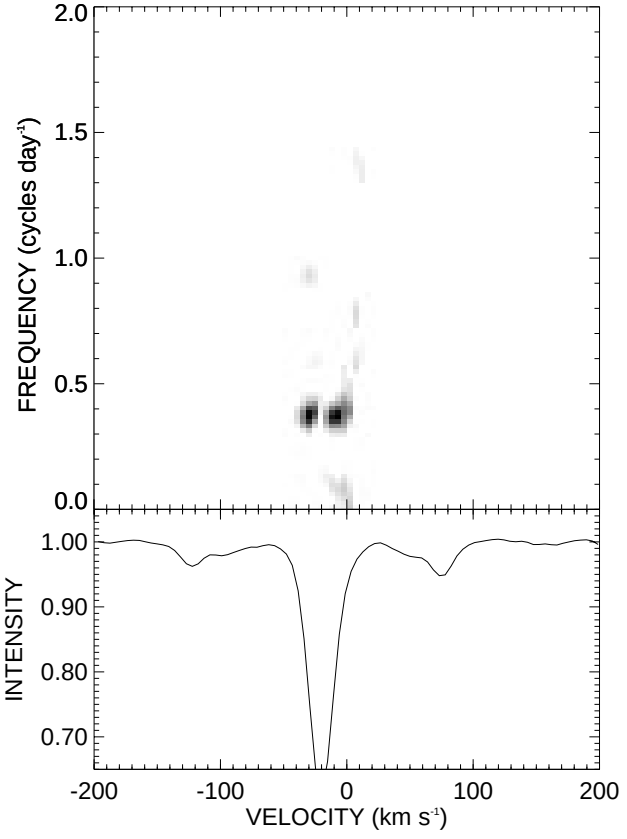

Figure 4. Periodogram for HR 8330 across the Fe II λ4508.289 line. Note the distribution of power across the line profile.

Table 3. HR 8330: results obtained from spectroscopic data.

Spectral line	Date range HJD−245 0000	n	Period (d)	Amplitude ($\mathrm{km\,s^{-1}}$)	T_v HJD−245 0000
Fe II λ4508	778–789	76	2.60	5.19	780.081
			±0.05	±0.13	±0.018
Ti II λ4501	778–789	76	2.62	5.23	780.074
			±0.06	±0.12	±0.018

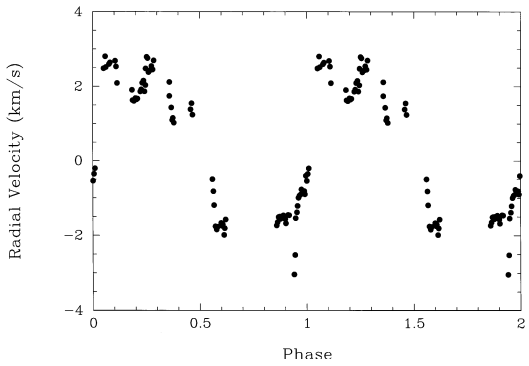

Figure 5. A phased relative radial velocity curve for HR 8330 based on the time series of first moments calculated from the Fe II λ4508.289 line profile. Phases are computed with the weighted mean values $T_v = 2\,450\,780.078$ and $P = 2.61$ d determined from Table 3.

the case in which the time of minimum brightness (our T_p) coincides with the time of maximum radius, which occurs at $V_{rad} = 0$ on the ascending branch of the radial velocity curve (our T_v). In the general case, we define the phase lag to be

$$\Delta\phi = \frac{T_p - T_v}{P}. \quad (2)$$

Using $T_p = 2\,450\,758.440$, $T_v = 2\,450\,780.078$, and $P = 2.593\,96$ d, we calculate the observed phase lag for HR 8330 is $\Delta\phi = 0.66 \pm 0.02$ ($= 237° \pm 7°$).

5 THE PHYSICAL CAUSE OF THE VARIABILITY

We investigate various mechanisms as possible explanations for the observed photometric and spectroscopic variability in HR 8330.

(1) Duplicity effects. The suspected γ Doradus variable HD 96008 (F0 V) was found to be an ellipsoidal variable with a 0.6-d period (Matthews 1990; Mantegazza & Poretti 1995). The 2.6-d period and shape of the light curve of HR 8330 also suggest ellipsoidal variation in this star. However, since the photometric and spectroscopic periods are identical within their errors, rather than differing by a factor of two, the observed variations *cannot* be due to the ellipticity effect.

(2) Spots. The rotational modulation of starspots (both hot and cool) was the last scenario to be rejected in the determination of the physical cause of variability among γ Doradus stars (see, e.g., Krisciunas et al. 1995; Hatzes 1998; Kaye et al., in preparation). In the case of HR 8330, we can also rule out the starspot hypothesis.

The observed correlation between radial velocity variation and rotation of spotted stars presented in Saar, Butler, & Marcy (1998) suggests that the radial velocity variations in HR 8330 are not the result of starspots. Using their fig. 2 and our $v \sin i$ of 9.1 km s^{-1}, we estimate that the predicted radial velocity amplitude (peak-to-peak) should be about 20 m s^{-1} if it were due to starspot activity. This predicted value is two full orders of magnitude smaller than the observed 5 km s^{-1} variation present in HR 8330.

(3) Pulsation. The period corresponding to the fundamental radial mode in early F dwarfs is of the order of hours; non-radial modes deriving their pulsational characteristics from pressure (*p*-modes) have still shorter periods. Only non-radial pulsation modes utilizing gravity as the restoring force (*g*-modes) can have periods compatible with the 2.61-d period of HR 8330 (Cox 1980). In addition, plasma motions arising from radial modes of various orders, along with non-radial *p*-modes, are dominated by vertical motions. Thus, in the 1-to-1 mapping from position across the stellar disc to position across the line profile, these pulsations have their maximum effect at line centre. Plasma motions resulting from *g*-mode pulsations, on the other hand, are dominated by horizontal motions (Cox 1980), resulting in large effects in the line wings. In Fig. 4 (above), it can clearly be seen that the distribution of signal power across the line profile is concentrated strongly in the wings with little or no contribution at line centre. This indicates that non-radial *g*-mode pulsation is the cause of the observed variations in HR 8330.

6 CONCLUDING PERSPECTIVE

We conclude that HR 8330 is a bona fide γ Doradus variable star based on the following: (1) its position in the HR diagram; (2) its identical photometric and spectroscopic periods, and (3) the physical mechanism of its variability. We have shown that the observed variations are the result of high-order (n), low-degree (ℓ), non-radial, *g*-mode pulsation.

This object does not have the longest period among the γ Doradus variables; the 2.89-d period of 9 Aurigae (Krisciunas et al. 1993, 1995; Zerbi et al. 1997; Kaye 1998) is the longest. HR 8330 does, however, have one of the largest amplitudes (0.024 mag in *B*) and is therefore an easier observational target than many other γ Doradus stars. With its single stable period, HR 8330 is one of an interesting subgroup within the γ Doradus variable class. Thus, it will be important to continue observations of HR 8330 to search for period, amplitude, and/or phase changes similar to those seen in other γ Doradus stars (see, e.g., Kaye & Zerbi 1997), as well as to understand better the physics behind the small-amplitude, non-periodic, radial-velocity variations (Fig. 5).

ACKNOWLEDGMENTS

ABK thanks Drs. Joyce Guzik and Paul Bradley for their helpful suggestions after reading various drafts of this manuscript. ABK also thanks NOAO for the travel grant that facilitated the time-series spectra. Many thanks go to Lou Boyd and Don Epand for their efforts to develop and operate Fairborn Observatory. Astronomy with automated telescopes at Tennessee State University has been supported by the National Aeronautics and Space Administration, most recently through NASA grants NCC2-977 and NCC5-228 (which funds TSU's Center for Automated Space Science), and the National Science Foundation, most recently through NSF grants HRD-9550561 and HRD-9706268 (which funds TSU's Center for Systems Science Research). This research has made use of the SIMBAD data base, operated at CDS, Strasbourg, France.

REFERENCES

Aerts C., 1996, A&A, 314, 115
Balona L. A., 1987, MNRAS, 224, 41
Balona L. A. et al., 1996, MNRAS, 281, 1315
Boesgaard A. M., Tripicco M. J., 1986, ApJ, 303, 724
Cowley A. P., 1976, PASP, 88, 95
Cox J. P., 1980, Theory of Stellar Pulsation. Princeton Univ. Press, Princeton NJ

Crawford D. L., 1975, AJ, 80, 955
Crawford D. L., Barnes J. V., Faure B. Q., Golson J. C., 1966, AJ, 71, 709
ESA, 1997, The Hipparcos Catalogue, Publ. SP-1200. ESA, Paris
Fekel F. C., 1997, PASP, 109, 514
Flower P., 1996, ApJ, 469, 355
Gray D. F., 1982, ApJ, 258, 201
Gray D. F., 1992, The Observation and Analysis of Stellar Photospheres. Cambridge Univ. Press, Cambridge
Gray R. O., Garrison R. F., 1989, ApJS, 69, 301
Hatzes A. P., 1998, MNRAS, 299, 403
Henry G. W., 1995, in Henry G. W., Eaton J. A., eds, Conf. Ser. 79, Robotic Telescopes: Current Capabilities, Present Developments, and Future Prospects for Automated Astronomy. Astron. Soc. Pac., San Francisco, p. 44
Högbom J. A., 1974, ApJS, 15, 417
Kaye A. B., 1998, PhD. thesis, Georgia State Univ.
Kaye A. B., Zerbi F. M., 1997, Delta Scuti Star Newsletter, 11, 32
Krisciunas K. et al., 1993, MNRAS, 263, 781
Krisciunas K., Griffin R. F., Guinan E. F., Luedeke K. D., McCook G. P., 1995, MNRAS, 273, 662
Mantegazza L., Poretti E., 1995, A&A, 294, 190
Matthews J., 1990, A&A, 229, 452
Saar S. H., Butler R. P., Marcy G. W., 1998, ApJ, 498, L153
Scarfe C. D., Batten A. H., Fletcher J. M., 1990, Publ. Dominion Astrophys. Obs., 18, 21
Stobie R. S., Whitelock P. A., eds., 1995, ASP Conf. Ser. 83, Astrophysical Applications of Stellar Pulsation. Astron. Soc. Pac.
Vaniĉek P., 1971, Ap&SS, 12, 10
Young R. K., 1945, Publ. David Dunlap Observatory, 1, 311
Zerbi F. M. et al., 1997, MNRAS, 290, 401
Zerbi F. M. et al., 1999, MNRAS, 303, 275

This paper has been typeset from a TEX/LATEX file prepared by the author.